

Direct Electron Transfer of Glucose Oxidase and Electrocatalysis of Glucose Based on Gold Nanoparticles/Electroactivated Graphite Nanocomposite

Murugan Velmurugan, Subramanian Sakthinathan, Shen-Ming Chen* Chelladurai Karuppiah

Electroanalysis and Bioelectrochemistry Lab, Department of Chemical Engineering and Biotechnology, National Taipei University of Technology, No.1, Section 3, Chung-Hsiao East Road, Taipei 106, Taiwan (R.O.C).

*E-mail: smchen78@ms15.hinet.net

Received: 18 April 2015 / Accepted: 24 May 2015 / Published: 24 June 2015

In this study, we reported a direct electron transfer reaction of glucose oxidase (GOx) at gold nanoparticles-electroactivated graphite/screen printed carbon electrode (AuNPs-EGr/SPCE). The activated graphite was prepared through a simple electrochemical activation method in the electrolyte medium containing 0.1 M KCl. The characterization of as-prepared electrocatalyst AuNPs-EGr was studied by scanning electron microscopy and elemental analysis. The enzyme GOx was immobilized on the surface of AuNPs-EGr modified SPCE by the drop casting method. The redox behavior of GOx/AuNPs-EGr/SPCE was clearly observed at a formal potential of -0.404 V with a peak separation (ΔE_p) of 42 mV which reveals that the fast electron transfer process has been observed between GOx and AuNPs-EGr modified SPCE. The modified electrode displayed very good linear response to glucose oxidation from 50 to 1600 μM with detection limit 2.5 μM and the sensitivity is 255 $\mu\text{AmM}^{-1}\text{cm}^{-2}$. The reported sensor exhibits a super selectivity and satisfactory reproducibility with good stability.

Keywords: Glucose biosensor, glucose oxidase, gold nanoparticles, graphite, screen printed carbon electrode

1. INTRODUCTION

The development of sensitive and selective electrochemical glucose biosensor have been focused in the past five decades because the accurate determination of blood glucose is very importance to control the diabetes. Glucose oxidase (GOx) and glucose dehydrogenase (GDH) are extensively used as a model enzymes for the sensitive and selective determination of glucose [1-3].

Recently, numerous metal nanoparticles such as silver, gold, palladium and platinum have been developed for the fabrication of glucose biosensor [4-7]. Among the various nanoparticles, gold nanoparticles (AuNPs) based nanocomposite have been focused in the recent years because of its biocompatible, large active sites, high electrical conductivity [8]. Moreover, numerous AuNPs based nanocomposite have been prepared and fabricated for the glucose biosensor by the various research group [9-11].

In order to increase the surface area with efficient catalytic activity of the AuNPs, some the supporting materials such as graphite, graphene and carbon nanotube have been used in the electrochemical sensor and biosensor application [11-15]. Interestingly, the electrochemically activated carbon nanomaterials have perceived to be an excellent supporting materials owing to their unusual electrochemical conductance along with excellent stability [16 & 17]. Relative to pristine graphite, the activated graphite possesses large active sites, higher electrical conductivity and excellent matrix for the incorporation of nanoparticles [13]. Moreover, the important feature of the electrochemical activated graphite is simple, biocompatible, time consuming, ecofriendly compare to other methods of activated graphite [17 & 18].

Recently, our research group focuses the preparation electrochemically activated graphite based metal and metal oxide nanomaterials for the fabrication of sensor and biosensor [13 & 19]. In our previous report, we have reported that AuNPs decorated activated graphite (AuNPs-AG) achieved excellent electrochemical catalytic activity in the detection of hydrazine sensor [13]. By motivating of this unusual properties of the AuNPs-AG, in this paper, we have fabricated glucose biosensor based on AuNPs decorated at electroactivated graphite (AuNPs-EGr) through simple electrochemical methods. GOx has been chosen as a typical enzyme for the fabrication of enzymatic glucose biosensor. The important features of our biosensor are simple, biocompatible, the easy covalent linkage between enzyme and nanocomposite, long-term stability. In addition, the demonstrated glucose biosensor achieved excellent electrochemical parameters such as wider linear range (50-1600 μM) and high sensitivity ($255 \mu\text{A}\text{mM}^{-1} \text{cm}^{-2}$) with the limits of detection of 2.5 μM .

2. EXPERIMENTAL

2.1. Chemicals and reagents

The raw graphite powder was obtained from Sigma–Aldrich and an average diameter of the graphite is about $>20 \mu\text{m}$. Screen printed carbon electrode was received from Zensor R&D Co., Ltd., Taipei, Taiwan. Potassium gold (III) chloride Trihydrate ($\text{KAuCl}_4 \cdot 3\text{H}_2\text{O}$) was purchased from Strem Chemicals (USA). Glucose oxidase and D (+) Glucose was obtained from Sigma–Aldrich. The phosphate buffer solution (0.05 M, pH 7) was prepared in doubly distilled (DD) water using Na_2HPO_4 and NaH_2PO_4 as a precursor solution. All the other solutions were made up by DD water without any further purification.

2.2. Apparatus

Throughout the study, the cyclic voltammetry (CV) experiments were performed by electrochemical workstation CHI 750a. For the morphological study, scanning electron microscopy (SEM) was taken by Hitachi S-3000H electron microscope. The elemental analysis (EDX spectrum) was by HORIBA EMAX X-ACT which was attached with Hitachi S-3000 H scanning electron microscope. Three electrochemical cell was used in the voltammetric studies such as screen printed carbon electrode (active surface area = 0.071 cm^2), saturated Ag/AgCl and a platinum electrode as a working, reference and an auxiliary electrode, respectively. All the experiments were performed in an inert atmosphere under ambient condition.

2.3. Fabrication of glucose biosensor using GOx/AuNPs-EGr/SPCE

Fabrication of AuNPs/EGr modified SPCE prepared through our previous method with little modification [13]. Briefly, first the graphite flake was dispersed in DMF solution (10 mg mL^{-1}) and then sonicated 15 min for uniform suspension. About $6 \mu\text{L}$ of dispersed graphite solution was drop cast on the pre-cleaned SPCE, then dried at $35 \text{ }^\circ\text{C}$. To activate the pristine graphite, the Gr/SPCE was immersed into electrolyte solution which containing 0.1 M KCl and further the potentiostat experiment was performed at 2.0 V for 200 s . After the preparation of EGr/SPCE, the AuNPs were deposited on EGr matrix in the presence of $1.3 \text{ mM KAuCl}_4 \cdot 3\text{H}_2\text{O}$ in $0.5 \text{ M H}_2\text{SO}_4$. The deposition of AuNPs was successfully carried out with a 5 consecutive cycles in the potential series from -0.2 to 1.3 V with the scan rate at 50 mV s^{-1} . The AuNPs deposited EGr/SPCE was slowly washed with DD water to eliminate the unbounded AuNPs and then dried for 10 min . To fabricate the biosensor, about $8 \mu\text{L}$ of GOx solution (5 mg mL^{-1}) was dropped on the AuNPs-EGr/SPCE and kept at $28 \text{ }^\circ\text{C}$ until its dried. The fabricated GOx/AuNPs-EGr/SPCE was used for the voltammetric experiments and it was also stored in pH 7 solution at $4 \text{ }^\circ\text{C}$ when rest of the experiments.

3. RESULTS AND DISCUSSION

3.1. Characterization

The morphological study of as-prepared AuNPs-EGr nanocomposite was carried out by SEM. Fig. 1 shows the SEM images of the pristine graphite flakes (A), EGr (B), AuNPs decorated EGr (C) and AuNPs deposited on ITO (inset of C). As can be seen in Fig. 1A and 1B, the smooth and more edged surface was clearly observed for pristine graphite and activated graphite, respectively. The pristine graphite was significantly edged through the electroactivation method, which direct to the exfoliation of pristine graphite into few layer graphite sheets. In addition, the SEM images of Fig. 1C show the AuNPs decorated graphite microsheets. It is uniformly distributed on the EGr surface and also the formation of AuNPs is a spherical in shape with an average size $\sim 70 \text{ nm}$. A similar morphological structure of AuNPs was observed while depositing on ITO (inset C) and pristine graphite (figure not

shown). Moreover, the AuNPs are well anchored on the electrochemically activated graphite microsheets which indicates that the more edge plane of the graphite sheets [20].

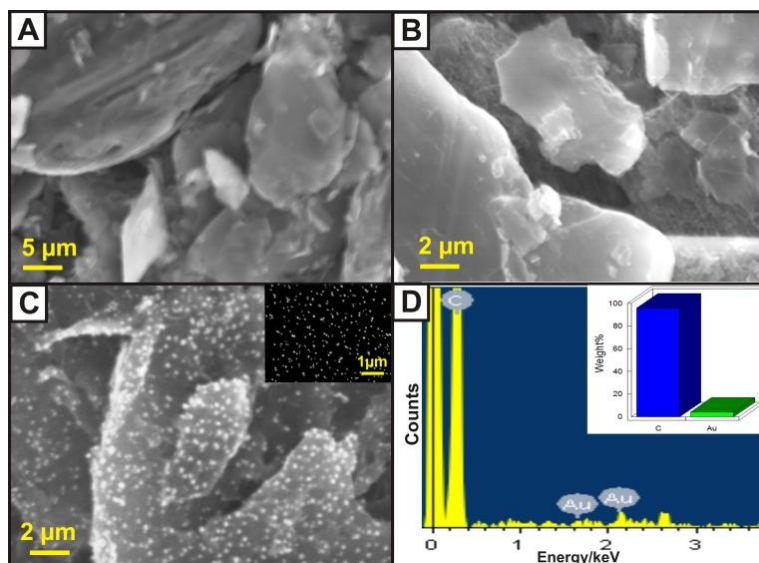


Figure 1. SEM images of (A) pristine graphite, (B) EGr, (C) AuNPs-EGr and (inset C) AuNPs. (D) EDX spectral data and (inset D) Quantitative elemental analysis of AuNPs-EGr nanocomposite.

The as-formed AuNPs-EGr nanocomposite is also characterized by EDX spectral analysis. Fig. 1D displays the EDX spectrum of AuNPs-EGr nanocomposite. A strong spectral peak for carbon was appeared at 0.32 keV. Besides, there is two other small peaks were obtained at 1.65 and 2.13 keV which is attributed to the formation of AuNPs on this composite. As can seen in inset Fig.1D, the elements are quantitatively analyzed and measured as 97.46 % of carbon and 2.65 % of Au. The above results confirmed that AuNPs are equally deposited on each EGr sheets to this nanocomposite.

3.2. Direct electrochemistry of GOx modified composite electrode

Direct electron transfer of GOx was evaluated at the different modified electrodes by the cyclic voltammetry method. Fig. 3 shows the CV results obtained for bare GOx/SPCE (a), GOx/AuNPs/SPCE (b), GOx/AuNPs-Gr/SPCE (c), GOx/EGr/SPCE (d) and GOx/AuNPs-EGr/SPCE (e) in N₂ saturated pH 7 solutions with a sweep rate at 50 mV s⁻¹. At bare GOx/SPCE, no obvious signal of GOx appeared due to the very poor immobilization of GOx on the SPCE surface. A very less electron transfer signal was observed on GOx/AuNPs/SPCE (b) which is also indicated the complicated immobilization of GOx on AuNPs. However, the redox couple was clearly obtained on GOx/AuNPs-EGr/SPCE (e) with a formal potential of -0.404 V and the ΔE_p of 42 mV which reveals that the fast electron transfer process has been observed between GOx and AuNPs-EGr modified SPCE. It is feature regarded as a characteristic reversible active center (FAD/FADH₂) of GOx, which

is responsible co-factor for the direct electron transfer through GOx and composite modified electrode [21].

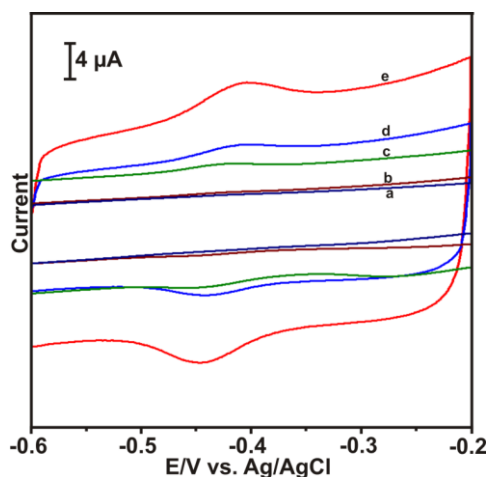


Figure 2. CV results obtained for the DET at different modified electrodes (a) GOx/SPCE, (b) GOx/AuNPs/SPCE, (c) GOx/AuNPs-Gr/SPCE, (d) GOx/Gr/SPCE and (e) GOx/AuNPs-EGr/SPCE at a sweep rate of 50 mV s^{-1} .

Compare with other graphite electrodes such as GOx/AuNPs-Gr/SPCE (c) and GOx/EGr/SPCE (d), the high peak current was observed only at the AuNPs-EGr modified SPCE. The AuNPs-EGr nanocomposite shows excellent electron transfer capability to promote the fast electron communication through GOx owing to the high conductivity and large edge plane defects of EGr sheets [20]. The ΔE_p at GOx immobilized AuNPs-EGr nanocomposite is smaller than the previously reported GOx based biosensors, indicating the fast direct electron transfer process of GOx [1, 22].

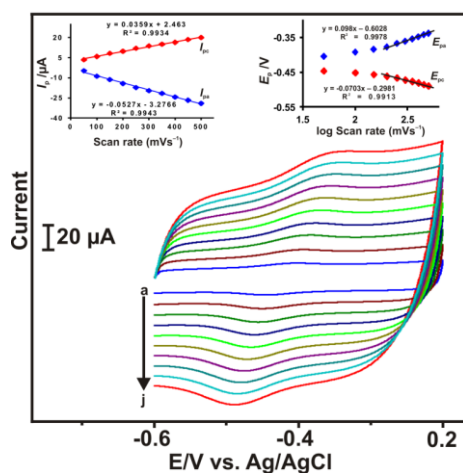


Figure 3. CVs for effect scan rate of GOx/AuNPs-EGr/SPCE in N_2 saturated electrolyte solutions at the different sweeping rates from 50 to 500 mV s^{-1} (a-j). The left inset shows the plot between I_p vs. scan rates and right side inset shows the plot between E_p vs. logarithm of scan rates.

Fig. 3 illustrates the CVs obtained to the effect of scan rates at GOx/AuNPs-EGr nanocomposite modified electrode in N₂ saturated pH 7 solution, the scan rate ranges from 50 to 500 mV s⁻¹. The anodic (*I*_{pa}) and cathodic (*I*_{pc}) peak currents were increased over the scan rate ranges from 50 to 500 mV s⁻¹ (a–j). Besides, the cathodic (*E*_{pc}) and anodic (*E*_{pa}) peak potentials was slightly shifted in lower sweeping rates (<200 mV s⁻¹), whereas no significant shift was observed at higher sweeping rates (>200 mV s⁻¹). The Δ*E*_p values are slightly increasing at higher sweeping rates. In addition, the inset (left side) of Fig. 3 confirms the linear behavior of both *I*_{pa} and *I*_{pc} in the rates of scanning ranges from 50 to 500 mV s⁻¹. The result indicates that the reversible manner of GOx on the AuNPs-EGr/SPCE is a surface-confined process [22]. The heterogeneous electron transfer rate constant (*k*_s) for GOx immobilized at AuNPs-EGr nanocomposite modified electrode is calculated by Laviron equation [23]. The two straight lines were obtained from the plot of *E*_{pc} and *E*_{pa} vs. logarithm of scan rates (Fig. 3 right side inset). Using Laviron theory, the electron transfer coefficient (*α*) value calculated to be 0.42, which is measured by the slope of those two straight lines of *E*_{pc} and *E*_{pa} such as -2.303RT/*α*nF and 2.303RT/(1-*α*)nF. According to the following equation (1), the *k*_s value of GOx immobilized AuNPs-EGr nanocomposite modified electrode was estimated to be 1.90 s⁻¹.

$$\log k_s = \alpha \log(1-\alpha) + (1-\alpha) \log \alpha - \log \frac{RT}{nFv} - \frac{\alpha(1-\alpha)nF\Delta E_p}{2.303RT} \quad (1)$$

The present GOx immobilized AuNPs-EGr/SPCE shows higher *k*_s value than that the other reported GOx based biosensors [24, 25 and 26]. The above result confirms AuNPs-EGr electrocatalyst assists the fast electron transfer between the GOx and SPCE surface.

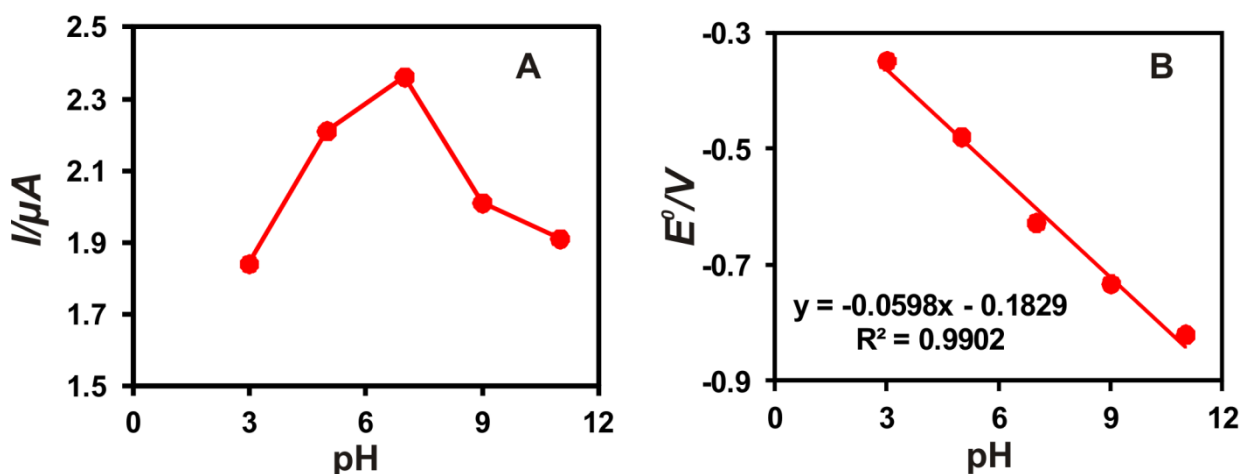


Figure 4. Influence of pH on GOx/AuNPs-EGr modified SPCE; **A)** The calibration plot of peak current vs. pH and **B)** the calibration plot of *E*⁰ vs. pH.

The influence of pH solution on the redox behavior of GOx immobilized AuNPs-EGr nanocomposite modified electrode is also carried out by CV in various pH solutions at the scan rate of 50 mV s⁻¹ (figure not shown). A pair of reversible peaks of GOx is clearly observed in each pH solution. Both *E*_{pc} and *E*_{pa} are shifted towards negative and/or positive direction while increasing and decreasing the pH range (pH 3–pH 11). The higher peak current of GOx/AuNPs-EGr/SPCE is

observed only on pH 7 solutions (Fig. 4A). Also, Fig. 4B shows the excellent linear behavior between the formal potential (E^0) of GOx and the pH range (pH 3–pH 11) with a slope value of -59.8 mV/pH. The above obtained slope value is almost equal to the theoretical value (-58.6 MV/pH) of the Nernstian equation, which indicating the identical number of protons (H^+) and electrons (e^-) involving electron transfer process [4]. Therefore, the result confirms that the DET of the redox couple at GOx is involving an equal number of protons (H^+) and electrons (e^-) transferred to the electrode surface. The electron transfer reaction of GOx/AuNPs-EGr/SPCE can be expressed by Eqn. 2 [4].

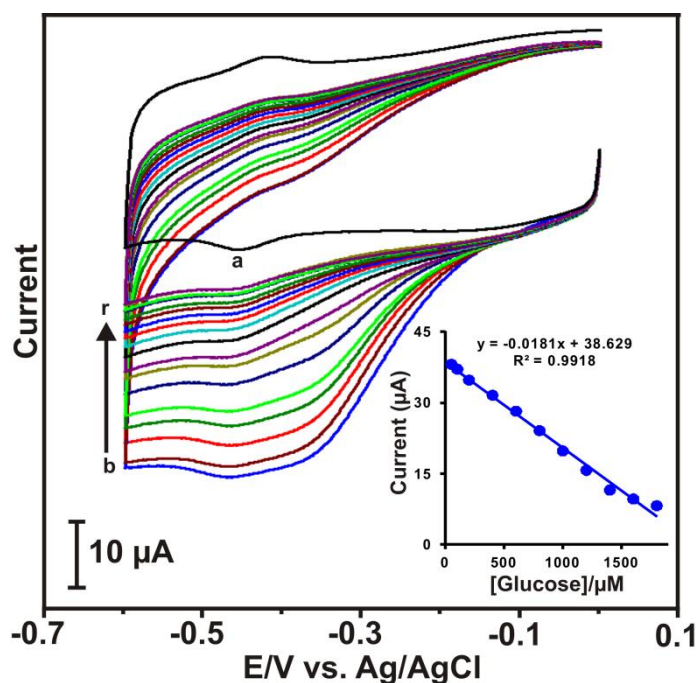
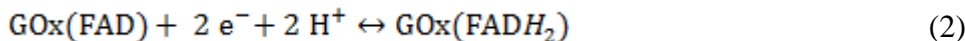


Figure 5. CVs of GOx/AuNPs-EGr/SPCE in N_2 saturated (a) and O_2 saturated PBS (pH 7) solution in various concentrations of glucose from 50 to 1800 μM at the scan rate of 50 $mV s^{-1}$, (b–r). The inset shows the calibration curve of I_p vs. glucose concentration.

3.3. Electrocatalysis of glucose on GOx/AuNPs-EGr/SPCE

The electrocatalysis of the GOx/AuNPs-EGr/SPCE was performed for the electro-oxidation of glucose molecule using CV. Fig. 4 displays the CV results of AuNPs-EGr nanocomposite modified electrode in O_2 saturated electrolyte solution (pH 7) with different concentrations of glucose (50–1800 μM) on the scan rate of 50 $mV s^{-1}$. As depicted in the CV results, the reduction peak current (I_{pc}) decreases whereas the oxidation peak current (I_{pa}) increases simultaneously leading to increase the concentration of glucose from 50 to 1800 μM . This is because of the decreasing the O_2 content in PBS solution as it is devoted in the glucose oxidation by the catalytic effect of GOx on the GOx/AuNPs-EGr modified SPCE [19]. The following equation can be expressed for the mechanism of glucose oxidation by GOx.



The I_{pc} was linearly decreased while increasing the glucose concentration and the linear range was obtained to be about 50–1600 μM (inset). The obtained linear regression equation is $I (\mu\text{A}) = -0.0181 + 38.629 c (\mu\text{M})$ with a correlation coefficient of 0.9918. The sensitivity and limits of detection (LOD) is calculated to be about $255 \mu\text{AmM}^{-1} \text{cm}^{-2}$ and $2.5 \mu\text{M}$ (S/N=3), respectively. The LOD of GOx/AuNPs-EGr modified electrode shows very lower than the other reported modified electrodes for the determination of glucose [1,5,24,27]. Hence, the fabricated biosensor exhibits very better analytical performance with higher k_s value than previously reported GOx immobilized AuNPs and carbon based nanocomposites modified electrodes. The developed glucose biosensor can be used for practicality measurements in the near future.

3.4. Selectivity, stability and reproducibility of the biosensor

Selective determination of glucose is significant in real time application of the biosensors. The neurotransmitters such as ascorbic acid dopamine and uric acid are cointerfering species with glucose detection in real sample analysis. For that reason, the effect of interference of the presented biosensor was evaluated by CV experiments. The response for glucose oxidation was observed at GOx/AuNPs-EGr nanocomposite modified electrode in pH 7 solution containing 2 mM glucose with 1 mM of interference such as AA, DA and UA (data not shown). Those interferences showed a negligible response that does not affect the glucose signal. The results suggested that the GOx/AuNPs-EGr/SPCE has proved good selectivity to detect the glucose in the presence of biological interference.

To evaluate the stability and reproducibility, GOx/AuNPs-EGr nanocomposite modified electrode was examined by CV. The fabricated GOx/AuNPs-EGr/SPCE was performed towards glucose. The GOx immobilized AuNPs-EGr nanocomposite modified electrode was stored at 4°C in pH 7 solution were not in use. Only 7.8 % of the signal is lost after 3 weeks, which indicates that GOx is highly active in this enzymatic biosensor. For the reproducibility, the five different GOx/AuNPs-EGr/SPCE was performed to analyze the glucose. The relative standard deviation (RSD) of the glucose oxidation with 2 mM glucose is calculated to be about 3.8 %. The above results further indicating that the GOx/AuNPs-EGr/SPCE has a very good stability and satisfactory reproducibility for the determination of glucose.

4. CONCLUSIONS

In conclusions, we have developed GOx/AuNPs-EGr/SPCE for the direct electron transfer reaction of GOx. Spherical structure of AuNPs was uniformly distributed on EGr surface which is confirmed from the SEM studies. Compare with pristine graphite, EGr shows higher edge plane defects and all the graphite sheets were uniformly edged by electroactivation. The redox peak current of GOx immobilized AuNPs-EGr nanocomposite modified electrode is about 2 and 2.2 folds higher than GOx/EGr/SPCE and GOx/AuNPs-Gr/SPCE, respectively. The fabricated biosensor shows a lower detection limit of $2.5 \mu\text{M}$ with the high sensitivity of $255 \mu\text{AmM}^{-1} \text{cm}^{-2}$ for the determination of

glucose. The developed GOx immobilized AuNPs-EGr/SPCE biosensor could be applicable for the analysis of glucose in practical and real time analysis.

ACKNOWLEDGEMENTS

This project was supported by the Ministry of Science and Technology and the Ministry of Education of Taiwan (Republic of China).

References

1. B. Liang, L. Fang, G. Yang, Y. Hu, X. Guo and X. Ye, *Biosens. Bioelectron.* 43 (2013) 131.
2. L. Hua, X. Wu and R. Wang, *Analyst*, 137 (2012) 5716.
3. M.N. Zafar, N. Beden, D. Leech, C. Sygmund, R. Ludwig and L. Gorton, *Anal. Bioanal. Chem.*, 402 (2012) 2069.
4. S. Palanisamy, C. Karuppiyah and S.M. Chen, *Colloids and Surf. B*, 114 (2014) 164.
5. K. Zhou, Y. Zhu, X. Yang and C. Li, *Electroanalysis*, 22 (2010) 259.
6. N. Cheng, H. Wang, X. Li, X. Yang and L. Zhu, *American J. Anal. Chem.*, 3 (2012) 312.
7. W. Liu, H. Wu, B. Li, C. Dong, M.M.F. Choi and S. Shuang, *Anal. Methods*, 5 (2013) 5154.
8. Y. Liu, and H.Y. Gu, *Microchim Acta*, 162 (2008) 101.
9. Y. Yu, Z. Chen, S. He, B. Zhang, X. Li and M. Yao, *Biosens. Bioelectron.* 52 (2014) 147.
10. J. T. Holland, C. Lau, S. Brozik, P. Atanassov, and S. Banta, *J. Am. Chem. Soc.*, 133 (2011) 19262.
11. H. Zhang, Z. Meng, Q. Wang and J. Zheng, *Sens. Actuators B*, 158 (2011) 23.
12. K. Zhou, Y. Zhu, X. Yang, J. Luo, C. Li and S. Luan, *Electrochim. Acta*, 55 (2010) 3055.
13. C. Karuppiyah, S. Palanisamy, S.M. Chen, S.K. Ramaraj and P. Periakaruppan, *Electrochim. Acta*, 139 (2014) 157.
14. R. Devasenathipathy, C. Karuppiyah, S.M. Chen, V. Mani, V.S. Vasantha and S. Ramaraj, *Microchim. Acta*, 182 (2015) 727.
15. J. Leng, W.M. Wang, L.M. Lu, L. Bai and X.L. Qiu, *Nanoscale Res. Lett.*, 9 (2014) 99.
16. S. Ku, S. Palanisamy, S.M. Chen, *J. Colloid Inter. Sci.*, 411 (2013) 182.
17. K. Parvez, Z.S. Wu, R. Li, X. Liu, R. Graf, X. Feng and K. Mullen, *J. Am. Chem. Soc.*, 136 (2014) 6083.
18. Z.Y. Xia, S. Pezzini, E. Treossi, G. Giambastiani, F. Corticelli, V. Morandi, A. Zanelli, V. Bellani and V. Palermo, *Adv. Funct. Mater.*, 23 (2013) 4684.
19. C. Karuppiyah, S. Palanisamy, S.M. Chen, V. Veeramani, P. Periakaruppan, *Microchim. Acta*, 181 (2014) 1843.
20. S. Palanisamy, R. Madhu, S.M. Chen and S.K. Ramaraj, *Anal. Methods*, 6 (2014) 8368.
21. S.J. Bao, C. M. Li, J.F. Zang, X.Q. Cui, Y. Qiao and J. Guo, *Adv. Funct. Mater.*, 18 (2008) 591.
22. X. Kang, J. Wang, H. Wu, I.A. Aksay, J. Liu and Y. Lin, *Biosens. Bioelectron.*, 25 (2009) 901.
23. E. Laviron, *J. Electronanal. Chem.*, 101 (1979) 19.
24. Q.L. Sheng, K. Luo, R.X. Liu and J.B. Zheng, *J. Chin. Chem. Soc.*, 59 (2012) 154.
25. A.G. Elie, C.H. Lei and R.H. Baughman, *Nanotechnology*, 13 (2002) 559.
26. Y.L. Yao and K.K. Shiu, *Electroanalysis*, 20 (2008) 1542.
27. S.H. Lim, J. Wei, J. Lin, Q. Li and J.K. You, *Biosens. Bioelectron.*, 20 (2005) 2341.